TU Delft

Delft University of Technology

Understanding the Flexibility Challenges of a Plant for Microbial CO2 Electroreduction with Hexanoic Acid Recovery

Luo, J.; Pérez-Fortes, Mar; Straathof, Adrie J.J.; Ramirez, Andrea

DOI
10.1021/acs.iecr.4c01385

Publication date
2024

Document Version
Final published version

Published in
Industrial and Engineering Chemistry Research

Citation (APA)
Luo, J., Pérez-Fortes, M., Straathof, A. J. J., & Ramirez, A. (2024). Understanding the Flexibility Challenges of a Plant for Microbial CO2 Electroreduction with Hexanoic Acid Recovery. *Industrial and Engineering Chemistry Research*, *63*(40), 17236-17251. https://doi.org/10.1021/acs.iecr.4c01385

Important note
To cite this publication, please use the final published version (if applicable).
Please check the document version above.

Copyright
Other than for strictly personal use, it is not permitted to download, forward or distribute the text or part of it, without the consent of the author(s) and/or copyright holder(s), unless the work is under an open content license such as Creative Commons.

Takedown policy
Please contact us and provide details if you believe this document breaches copyrights.
We will remove access to the work immediately and investigate your claim.

This work is downloaded from Delft University of Technology.
For technical reasons the number of authors shown on this cover page is limited to a maximum of 10.

I&EC research
Industrial & Engineering Chemistry Research

Open Access
This article is licensed under CC-BY 4.0

pubs.acs.org/IECR
Article

Understanding the Flexibility Challenges of a Plant for Microbial CO_2 Electroreduction with Hexanoic Acid Recovery

Jisiwei Luo,* Mar Pérez-Fortes, Adrie J. J. Straathof, and Andrea Ramirez

Cite This: *Ind. Eng. Chem. Res.* 2024, 63, 17236−17251
Read Online

ACCESS | Metrics & More | Article Recommendations | Supporting Information

ABSTRACT: CO_2 electroreduction driven by renewable energy is a promising technology for defossilizing the chemical industry, but intermittency challenges its operation. This work aims to understand the impacts of intermittency on the design, volume flexibility, and scheduling of a microbial electrosynthesis (MES) plant that converts CO_2 to hexanoic acid. A battery and a storage tank were considered to buffer the intermittency. Explorative case studies showed that batteries were economically unfavorable. Restricted by the downstream processing (DSP) flexibility, a storage tank with optimized size combined with optimal scheduling, under the assumed conditions in this work, improved the plant's volume flexibility only by 10%. The carbon footprint became 3 times lower when switching from grid to renewable electricity, but the levelized production cost of hexanoic acid increased. Hence, coupling with renewable electricity was not economically but environmentally favorable. Developing more flexible DSP technologies or synthesizing higher-purity chemicals are needed to enhance MES's attractiveness.

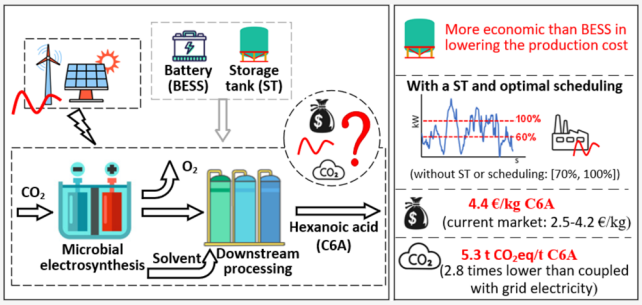

Downloaded via TU DELFT on October 14, 2024 at 11:39:47 (UTC).
See https://pubs.acs.org/sharingguidelines for options on how to legitimately share published articles.

1. INTRODUCTION

To mitigate anthropogenic global warming, accelerating energy transitions is crucial in many industrial sectors, including the chemical sector.[1,2] To reduce CO_2 emissions in the chemical sector, fossil-based feedstocks and fuels are expected to be replaced by cleaner alternatives. For instance, fossil-based carbon sources can be replaced by CO_2 captured from the air or exhaust gas, while fossil-based electricity can be substituted by renewable energy, such as solar and wind. Therefore, the electroreduction of CO_2 to value-added chemicals with renewable electricity is a promising alternative in the chemical sector. It is also seen as a prospective candidate for demand response by the power sector.[3,4] Among the different CO_2 electroreduction technologies, microbial electrosynthesis (MES) is an emerging technology that can convert CO_2 into useful chemicals through electricity-driven microbial reactions, such as hexanoic acid.[5−7] High-purity hexanoic acid has a high market value and is, hence, an attractive product. It is currently produced by fractional distillation of coconut or palm kernel oil, mainly exported by Indonesia or Malaysia.[8,9] As a result, this product is constrained by the origins and availability of raw materials, whereas the MES route would allow for more flexible supply chains and upscaling.

Up to now, both fundamental research and ex-ante technoeconomic assessments of low-temperature direct CO_2 electroreduction technologies, focus on the synthesis of commodity chemicals or fuels such as hydrogen, methane, methanol, or ethylene.[10−12] Their downstream recovery and purification processes are challenging because of the low concentration of the targeted products and the type of impurities. However, downstream processing (DSP) is often less emphasized or is even overlooked in ex-ante technoeconomic assessments.[13] MES produces hexanoic acid in a dilute aqueous environment. Hexanoic acid has a longer carbon chain and, hence, a higher boiling point. Additionally, they can form an azeotrope with water. As a result, the reported separation trains cannot easily recover it to a high degree of purity.[14−16] Moreover, the intrinsic variability in renewable electricity and consequent fluctuations in the throughput rate of the MES unit further exacerbate the challenge in the DSP design. Some researchers have investigated the performances of MES technologies under fluctuating renewable electricity supply, at a lab or plant scale.[17−20] However, hexanoic acid was not their target product.

In our previous work,[21] we proposed and modeled a MES plant producing high-purity hexanoic acid at a design capacity of ca. 10 kt/y and consuming 602 TJ/y of electricity. The DSP technologies selected to purify the hexanoic acid stream were liquid−liquid extraction (LLE), solvent regeneration (SR), and distillation. We assessed the plant's volume flexibility (under-

Received: April 11, 2024
Revised: September 13, 2024
Accepted: September 13, 2024
Published: September 24, 2024

ACS Publications
© 2024 The Authors. Published by American Chemical Society

https://doi.org/10.1021/acs.iecr.4c01385
Ind. Eng. Chem. Res. 2024, 63, 17236−17251

Table 1. Overview of Case Studies[a]

	reference		explorative			optimized
case (k)	A	B	C	D	E	F
Factors Considered						
electricity profile	grid	IRE	IRE	IRE	IRE	IRE
buffering units implemented	-	-	BESS	ST	BESS&ST	depends
predefined sizes of buffering units	-	-	yes	yes	yes	-
predefined operating scheme	-	-	yes	yes	yes	-
optimized scheduling	-	-	-	-	-	yes
optimized sizes of buffering units	-	-	-	-	-	yes
Indicators Used						
production shutdown time per year (h/y)	-	yes	yes	yes	-	yes
hexanoic acid production (kt/y)	-	yes	yes	yes	-	yes
levelized production cost of hexanoic acid, LPC^{k}_{C6A} (€/kg)	yes	yes	yes	yes	-	yes
load ratio range, LRR^{k} (%)	-	yes	yes	yes	-	yes
total electricity consumption EC^{k}_{ttl} (%)	-	yes	yes	yes	-	yes
surplus electricity consumption EC^{k}_{spl} (%)	-	-	yes	-	-	depends
extra production required, $\dot{M}_{C6A,xr}$ (kt/y)	-	-	-	-	yes	-
extra production available, $\dot{M}_{C6A,xa}$ (kt/y)	-	-	-	-	yes	-
carbon footprint (t CO_2eq/t C6A)	yes	yes	-	-	-	yes

[a]IRE: intermittent renewable electricity; BESS: battery energy storage system; ST: storage tank.

stood as the ability of the plant to operate over a range of electricity loads while meeting product requirements, and not damaging the equipment)[22] for different intermittent renewable electricity (IRE) profiles and storage strategies with batteries. According to our modeling results, the MES plant without a battery energy storage system (BESS) could be operated between 70 and 100% of its nominal capacity. The major bottleneck was the last heat-based distillation unit in the process. Below 70%, the plant must be shut down. The results suggested that covering short periods of electricity shortage by a BESS increased the product quantity synthesized yearly, though the reduction in the production cost was insignificant (e.g., with a BESS size under 14 MW). On the other hand, covering long periods of electricity shortage was too capital-intensive; the capital investment in the BESS soared because of the substantial capacity required, whereas limited extra revenue was obtainable. For instance, to avoid all shutdown periods, a BESS of nearly 500 MW would have been needed. Based on the outcome of our previous work,[21] which investigated different predefined sizes and operating schemes of the BESS (discrete cases), we argued that if a capital-intensive flexibility strategy is not used efficiently, it can lead to a high sunk cost. Optimizing the sizes of the buffering units, the use of the buffering units, and the operating loads of the MES plant were deemed necessary. In contrast to the expensive BESS, a cheaper buffering option, storage tanks (ST), has been advised in the literature to decouple the more from the less flexible sections of a process, to buffer the fluctuations in flow rates caused by intermittent renewable electricity in Power-to-Chemical plants.[11,23−27]

Operation scheduling has been primarily intended for meeting product demand and reducing capital and operating costs.[28,29] However, in recent years, integrating IRE into the electricity grid while minimizing operating costs has led to a considerable and growing number of studies, which have approached the IRE integration problem as a scheduling problem with a commonly used hourly resolution over a year.[1,27,30−35] Such a problem has usually been formulated as a mixed-integer linear programming (MILP) or a mixed-integer nonlinear programming (MINLP) problem.

In this paper, we extend our previous work[21] by addressing two questions of relevance for stakeholders and technology developers: (i) how does hourly fluctuation in the electricity supply affect the sizing of the buffering units (i.e., BESS and ST) and scheduling of a MES plant? and (ii) what are the subsequent trade-offs in terms of technoeconomic performances and carbon emissions when the buffering units are installed and the scheduling is optimized? We aim to provide insights into the flexible operation of Power-to-Chemical processes that synthesize long-chain chemicals.

2. MATERIALS AND METHODS

This work started with building the system model, where the design considerations of the plant were specified, the process model was developed, and electricity profiles were selected (Section 2.1). Next, explorative case studies were conducted under predefined operating schemes and buffering unit sizes (Section 2.2), which were the starting point of the optimization problem. They helped to narrow the optimization down, namely reducing several variables and nonlinearities, which eventually determined the use of a ST as the only buffering unit and confined the boundaries of variables. Section 2.3 elaborates on how these cases were characterized by various indicators. Next, an MINLP (i.e., mixed-integer quadratically constrained programming-MIQCP) problem was constructed and solved in Python (Section 2.4). The operating patterns of the MES-based plant and of the tank and the size of the tank were optimized to obtain maximum annualized net profit (ANP). This optimized case was further evaluated by using several indicators presented in Section 2.3. In addition, the carbon footprint was calculated for the optimized case and compared with the cases with grid electricity and continuous operation and with IRE but without buffering units (see Section 2.5), revealing the impacts of IRE as well as of the optimal scheduling and buffering unit size on the carbon footprint. Last, sensitivity analyses were performed on the optimized case (Section 2.6).

Table 1 gives an overview of the six (reference, explorative, and optimization) cases studied in this work (details in Section 2.2). For clarification, Cases A, B, and C are the same as Cases

https://doi.org/10.1021/acs.iecr.4c01385
Ind. Eng. Chem. Res. 2024, 63, 17236−17251

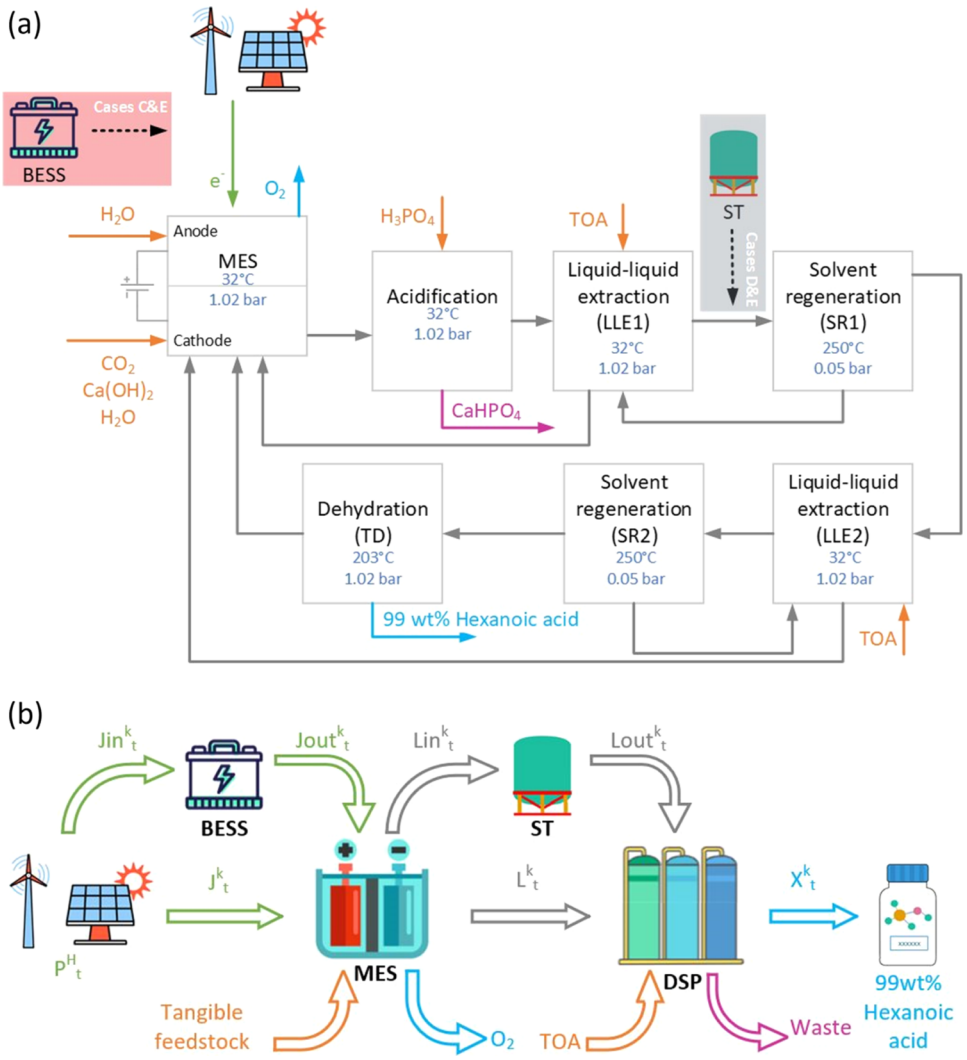

Figure 1. (a) Block flow diagram of the process of hexanoic acid production via MES. MES: microbial electrosynthesis. BESS: battery energy storage system. LLE: liquid−liquid extraction. SR: solvent regeneration. TD: dehydration column. ST: storage tank. TOA: trioctylamine. (solvent used for liquid−liquid extraction). (b) A simplified illustration of the operating patterns of the MES plant. Notice: the acidification unit was omitted in this figure. DSP: downstream processing. Adapted with permission from ref 21, Copyright 2024 Chemical Engineering Research and Design.

0, 2, and 4 in our previous work,[21] respectively. Moreover, it summarizes various indicators used in this work for characterizing the performances of the different cases (details in Sections 2.3 and 2.5).

2.1. System Model. *2.1.1. Design Considerations.* The MES plant was assumed to be installed in the Port of Rotterdam and to have a lifetime of 30 years. It produces 99 wt % hexanoic acid as the main product at a nominal production rate of ca. 10 kt/y (at a continuous operation, 8760 h/y) and ca. 22 kt/y of compressed O_2 as a byproduct. Its configuration is described in Section 2.1.2.

2.1.2. Process Description. Figure 1a is a simplified block flow diagram of the MES plant. Demineralized H_2O is fed into the anode chamber of the MES, and the byproduct, O_2, is produced. Demineralized H_2O, CO_2, $Ca(OH)_2$, and electrons are supplied to the cathode chamber, where carboxylates and the corresponding carboxylic acids are generated. The stream is then sent to the DSP units for acidification, filtration, recovery via two LLE units with distillation-based SR, and final distillation-based dehydration to obtain the 99 wt % hexanoic acid.

2.1.3. Electricity Profiles. Two electricity profiles were selected and used. One was constant grid electricity provided at the plant's nominal capacity. It was assumed to be sold to the MES plant at the average industrial electricity price in The Netherlands in 2019.[36] The second profile was a hybrid IRE, consisting of combined solar and wind power. This profile has an hourly resolution and was generated based on the wind speed and solar radiation in the region of Rotterdam in 2019. As a design condition, the average hourly capacity of the hybrid farms (i.e., solar and wind farms) was set at 200% of the nominal hourly electricity consumption rate of the MES plant. The Supporting Information (SI) explains how the profile was generated and its corresponding pricing scheme.

2.2. Case Specification. *2.2.1. Case A.* This is the first reference case where the plant was powered by constant grid electricity and operated at its nominal conditions, and no buffering unit was installed.

2.2.2. Case B. This is the second reference case, where the plant was driven by hybrid IRE while no buffering unit was deployed. For the operation of the plant, it was assumed that when the available electricity from the hybrid farms could not

https://doi.org/10.1021/acs.iecr.4c01385
Ind. Eng. Chem. Res. 2024, 63, 17236−17251

enable the production at the plant's minimum tolerable throughput rate, which is 70% of its nominal capacity, the plant was shut down. On the other hand, if the available electricity was higher than the plant's maximum tolerable electricity load, which is 100% of its nominal capacity, the production was kept at its maximum capacity and the surplus electricity available (the amount of electricity that exceeds the plant's nominal electricity consumption rate) was not used.

2.2.3. Case C. This is an explorative case where the plant was driven by hybrid IRE, and a BESS was installed before the MES unit (Figure 1a). The plant's operating scheme was predefined, and the BESS capacity was varied.

Based on the range of tolerable capacities mentioned for Case B, at each BESS capacity studied, the plant's operating scheme was defined by the following sequential rules (schematically depicted in the SI).

(1) When the total electricity available from the hybrid IRE and the BESS does not reach the minimum tolerable electricity power of the plant, which is 70% of its nominal capacity, shut down the production of hexanoic acid;
(2) otherwise, ensure the production at the plant's minimum tolerable throughput rate, if needed, with the stored electricity from the BESS;
(3) if the BESS is not fully charged and not used for production, charge it. It is possible that the BESS is charged while the production is off because of insufficient electricity to reach the plant's minimum tolerable throughput rate;
(4) if the BESS is fully charged, increase the production of hexanoic acid using hybrid IRE directly up to the plant's maximum throughput rate, which is 100% of its nominal capacity;
(5) electricity that cannot be consumed (because the BESS is fully charged and the plant is working at 100% of its nominal capacity) is not used by the MES plant.

Moreover, we assumed that, (1) at the start of operation (t = 1), the BESS was already fully charged; (2) the BESS could be charged or discharged up to its full capacity within 1 h; (3) consistent with ref 21, for each equipment, the material flow rate was linear to the electricity consumption rate. As measured in ref 21, the consumption rate of utility (i.e., heating and chilling) was nonlinear to the material flow rate due to the penalties for deviating from the nominal operating conditions.

2.2.4. Case D. In this explorative case, the plant was driven by the hybrid IRE and a ST was implemented in front of the SR1 (Figure 1a) to decouple the more flexible section (i.e., units prior to the ST) from the less flexible section (i.e., units after the ST) of the process. This location was proposed based on the fact that the heat-based columns were limiting fluctuations handling and SR1 is the first heat-based column in the plant.[21] The plant's operating scheme was predefined, and the ST size was varied.

Based on the range of tolerable capacities of Case B, at each ST size studied, the plant's operating scheme was specified by the sequential rules below (schematically depicted in the SI):

(1) when the electricity available from the hybrid IRE and the intermediate chemicals stored in the ST together cannot enable the plant's minimum tolerable throughput rate, shut down the production;
(2) otherwise, ensure the production at the minimum tolerable throughput rate of the plant, if needed, with the stored intermediate chemicals from the ST;
(3) if the ST is not fully filled and the intermediate chemicals stored inside it are not used for production, fill it. It is possible that the production is off due to insufficient flow going to SR1, however, the MES can consume electricity and the intermediate chemicals produced are stored in the ST;
(4) when the ST is fully filled, increase the production without using the stored chemicals from the ST until the plant's maximum throughput rate, which is 100% of its nominal capacity;
(5) electricity that cannot be consumed (because the ST is fully filled, and the plant is working at 100% of its nominal capacity) is not used by the MES plant.

Note that the intermediate chemicals stored in the ST could essentially be seen as "stored electric energy", which was the electricity available from the hybrid farms previously and used by MES to generate product compounds and then stored in the chemical bonds.

Moreover, we assumed that, (1) at the start of operation (t = 1), the ST was already fully filled; (2) the ST could be filled or drained up to its full capacity within 1 h; (3) same as the third assumption for Case C; (4) electricity was all consumed by the more flexible section of the process and utility was all consumed by the less flexible section of the process for simplicity, which was supported by the results in ref 21, where only 1.5% of electricity was consumed in the less flexible section and only 1% of the utility was used in the more flexible section. See the SI (Section 6) for a check of this hypothesis.

2.2.5. Case E. In this last case study, the plant was driven by hybrid IRE and a BESS and a ST were implemented at the same plant locations as in Cases C and D, respectively. This case study aimed to understand if the two buffering units would have synergies and further promote the production quantity of hexanoic acid and the economic performance of the plant. Since storage tanks are usually much cheaper than batteries, we explored the potential advantages of deploying a BESS in addition to a ST of the size that yielded the best economic performance in Case D, to assess if the BESS unit can enable extra hexanoic acid production to pay back its capital costs and even improve the operating income.

First, we calculated how much extra production of hexanoic acid was required per year "$\dot{M}_{C6A,xr}$" to pay back each GJ/h of BESS implemented when the ST was already in place. Then, we calculated how much extra production per year "$\dot{M}_{C6A,xa}$" was available per GJ/h of BESS implemented in addition to this ST (see equations in Section 2.3.4).

The operating scheme when BESS and ST were implemented concurrently was also predefined. This scheme was based on the assumption that the BESS should be used more frequently so it could consume more electricity (that otherwise will not be used) to boost the production of hexanoic acid.[21] At each BESS capacity studied, the plant's operating scheme followed the sequential rules below (schematically depicted in the SI):

(1) when the electricity available from hybrid IRE, the stored electricity in the BESS, and the intermediate chemicals stored in the ST cannot enable together the plant's minimum tolerable throughput rate, the production is shut down;

https://doi.org/10.1021/acs.iecr.4c01385
Ind. Eng. Chem. Res. 2024, 63, 17236−17251

(2) otherwise, ensure the production at the plant's minimum tolerable throughput rate, if needed, with stored electricity from the BESS and/or the stored chemicals from the ST;

(3) if the ST is not fully filled and the intermediate chemicals stored inside are not used for production, fill it. It is possible that the production is off due to insufficient flow going to SR1, however, the MES can still consume electricity and the intermediate chemicals produced can be stored into the ST. When the ST is full and the first rule still cannot be achieved, the BESS can be charged;

(4) when the ST is fully filled, increase the production of hexanoic acid without using the stored chemicals from the ST until the plant reaches its maximum throughput rate, i.e., 100% of its nominal capacity. If the hybrid IRE does not reach 100% of the plant's nominal electricity load, stored electricity in the BESS shall be used. If the hybrid IRE is over 100% of the plant's nominal electricity load, and the BESS is not fully charged, charge the BESS;

(5) electricity that cannot be consumed (because the BESS is fully charged, the ST is fully filled, and the plant is working at 100% of its nominal capacity) is not used by the MES plant.

The assumptions made are consistent with those of Cases C and D.

2.3. Technoeconomic Evaluation. The process model was first developed at nominal conditions and a continuous operation in Aspen Plus.[21] The mass and heat balances of the process at different throughput rates were retrieved from Aspen Plus and combined with a buffering unit, the hybrid IRE profile, and an operating scheme by using Python scripts, where the indicators described in this section were calculated.

2.3.1. Levelized Production Cost. The leveled production cost of hexanoic acid (LCA_{C6A}) is calculated using eqs 1−3. Costs include capital expenditure (CAPEX) and operating costs (OPEX). CAPEX of the plant is a sum of direct costs, indirect costs, and working capital. Direct costs are the purchase costs of all physical items, estimated based on the Aspen process model. Values were retrieved from Aspen Process Economic Analyzer v12, webpages, or the literature. Indirect costs and working capital were estimated according to heuristics[37−39] expressed as a series of percentages of purchase costs. OPEX is classified into five categories: operation and maintenance, feedstock, utilities (i.e., heating and chilling), waste treatment, and electricity. Operation and maintenance costs are associated with the purchased costs as well as labor costs and were calculated according to the above-mentioned heuristics. Feedstock and waste treatment costs were based on mass balances and material prices. Utilities and electricity prices were obtained from The Netherlands. A discount rate of 8% was assumed over the lifetime of 30 years. The plant would depreciate over 30 years and a salvage rate of 3.3% of the initial CAPEX was considered. Since the plant has a salvage value and some equipment (i.e., LLE & BESS) will be replaced after 15 years, CAPEX varies along the time. The construction of the plant was assumed to last for a year.

Considering that the byproduct O_2 was produced at a higher quantity than hexanoic acid, an economic allocation between hexanoic acid and O_2 was applied to both indicators (AF_{C6A}). The selling prices of hexanoic acid and O_2 were based on literature.[40,41] More details about the economic inputs and heuristics used are provided in SI.

$$\mathrm{LPC}^{k}_{\mathrm{C6A}} = \frac{\mathrm{AF}_{\mathrm{C6A}} \sum_{y=1}^{n^{\mathrm{plant}}} \frac{\mathrm{CAPEX}^{k}_{y} + \mathrm{OPEX}^{k}}{(1+r)^{y}}}{\sum_{y=1}^{n} \frac{\dot{M}^{k}_{\mathrm{C6A}}}{(1+r)^{y}}} \tag{1}$$

$$\mathrm{OPEX}^{k} = O\&M^{k} + F^{k} + UT^{k} + WT^{k} + E^{k} \tag{2}$$

$$\mathrm{AF}_{\mathrm{C6A}} = \frac{\dot{M}^{\mathrm{A}}_{\mathrm{C6A}}\theta_{\mathrm{C6A}}}{\dot{M}^{\mathrm{A}}_{\mathrm{C6A}}\theta_{\mathrm{C6A}} + \dot{M}^{\mathrm{A}}_{\mathrm{O_2}}\theta_{\mathrm{O_2}}} \tag{3}$$

2.3.2. Load Ratio Range. The load ratio range (LRR) was used to quantify the volume flexibility at the plant level. It was defined in our previous work[21] as the amount of available electricity (unit: GJ/h) from the hybrid farms that the plant could fully consume while meeting product requirements (i.e., purity and recovery rate) without damaging the equipment, divided by the plant's nominal electricity consumption rate (unit: GJ/h). Hence, the boundaries of the LRR are expressed in percentages, and a precision of 1% was used. The formulas for calculating the LRR (see eq 4) were proposed in our previous work[21] and are slightly modified and briefly explained below with the help of Figure 1b.

First of all, the LRR is calculated using the power profile and outcome operating profiles over a year with a time resolution of one h (i.e., 8760 h). In the first step, based on the annual power profile of the hybrid farms "P^{H}_{T}", at each power "v" generated by the farms, the total number of hours were counted together using an Iverson bracket (see eq 4). Then, based on the resulting operating profiles of the plant, the number of hours were counted at each electricity power "v" if the plant can meet two expectations simultaneously: (1) fully consume the available electricity "$\mathrm{Jin}^{k}_{t} + J^{k}_{t} = v = P^{H}_{t}$" from the hybrid farms and (2) produce hexanoic acid "$X^{k}_{t} \geq 0.7X_{o}$" (0.7 is explained in the following paragraph). Next, at each electricity power, a percentage of "C^{k}_{v}" was calculated using the two counts. This percentage represents how frequently the plant can be operated with the two expectations met when the electricity power is "v". This percentage is denoted as the coverage percentage hereafter. If the coverage percentage is 100% at a particular "v", it means that the plant can always operate as expected when "v" is supplied from the hybrid farms. Finally, a continuous range of electricity power was identified, where the corresponding coverage percentages were all 100%.

$$LRR^{k} = [\min V^{k}_{LB}, \max V^{k}_{UB}] \tag{4}$$

s.t.

$$T = [1, 8760] \cap \mathbb{Z}$$

$$C^{k}_{v} = \frac{\sum_{t\in T}[\![Jin^{k}_{t} + J^{k}_{t} = v = P^{H}_{t}, X^{k}_{t} \geq 0.7X_{o}]\!]}{\sum_{t\in T}[\![P^{H}_{t} = v]\!]} \quad ,\forall v \in P^{H}_{T}$$

$$V^{k}_{LB} = \{\frac{v}{J_o} | v \leqslant J_{min}, C^{k}_{\forall v^{*}\in[v, J_{min}]} = 100\%\}$$

$$V^{k}_{UB} = \{\frac{v}{J_o} | v \geqslant J_{max}, C^{k}_{\forall v^{*}\in[J_{max}, v]} = 100\%\}$$

The LRR of Cases A and B was [70%, 100%] based on ref 21. It means that during any hour in which the available electricity from the hybrid farms was between 70 and 100% of the process's nominal electricity consumption, the plant could take in all the available electricity while safely producing hexanoic acid. Below 70%, there was an electricity shortage, and the plant had to be shut down. Above 100%, without a BESS or

https://doi.org/10.1021/acs.iecr.4c01385
Ind. Eng. Chem. Res. 2024, 63, 17236−17251

ST, the surplus electricity available from the hybrid farms could not be used by the plant.

2.3.3. Total and Surplus Electricity Consumption. Total and surplus electricity consumptions were distinguished. Both are cumulative indicators and are expressed as percentages. During the calculation, both numerators and denominators were summed per annum or by specific available electricity power generated by the hybrid farms. The detailed explanations are as follows. The total electricity consumption "EC^k_{ttl}" is the electricity taken in by the plant "$Jin^k_t + J^k_t$" divided by the available electricity power from the hybrid farms "P^H_t" (see Figure 1b). The surplus electricity consumption "EC^k_{spl}" focuses on the plant's surplus electricity consumption "$Jin^k_t + J^k_t - J_o$" and the surplus available electricity "$P^H_t - J_o$" from the hybrid farms. "J_o" is the nominal electricity load of the plant. Equations 5 and 6 show how these two indicators are summed per annum "T", respectively. Equations 7 and 8 show how these two indicators can be summed by a specific available electricity power generated by the hybrid farms "v", respectively.

$$EC^k_{ttl} = \frac{\sum_{t\in T} Jin^k_t + J^k_t}{\sum_{t\in T} P^H_t} \quad T = [1, 8760] \cap \mathbb{Z} \tag{5}$$

$$EC^k_{spl} = \frac{\sum_{t\in T} (Jin^k_t + J^k_t - J_o)[\![P^H_t > J_o]\!]}{\sum_{t\in T} (P^H_t - J_o)[\![P^H_t > J_o]\!]} \quad T = [1, 8760] \cap \mathbb{Z} \tag{6}$$

$$EC^k_{ttl} = \frac{\sum_{t\in T} v[\![Jin^k_t + J^k_t = P^H_t = v]\!]}{\sum_{t\in T} v[\![P^H_t = v]\!]} \quad \forall v \in P^H_T \tag{7}$$

$$EC^k_{spl} = \frac{\sum_{t\in T} (v - J_o)[\![Jin^k_t + J^k_t = P^H_t = v > J_o]\!]}{\sum_{t\in T} (v - J_o)[\![P^H_t = v > J_o]\!]} \tag{8}$$

2.3.4. Extra Production Required and Available. As mentioned in Section 2.2.5, two extra indicators were specially used for Case E. The extra production required "$\dot{M}_{C6A,xr}$" was calculated using eq 9. The capital cost of the BESS was annualized to the equivalent annualized cost (EAC) using eqs 10 and 11. The extra production available "$\dot{M}_{C6A,xa}$" was calculated based on the extra electricity the BESS can consume when the ST was already deployed. The extra electricity that the BESS could consume from the hybrid IRE was calculated when applying the operating scheme in Section 2.2.5. Then, it was translated into "$\dot{M}_{C6A,xa}$" using eq 12.

$$\dot{M}_{C6A,xr} = \frac{EAC^{BESS} + O\,\&\,M^{BESS}}{\min LPC^{D}_{C6A} - \frac{(F^A + WT^A + E^A + UT^A)}{\dot{M}^{A}_{C6A}}} \tag{9}$$

$$EAC^i = \frac{CAPEX^i}{\varphi^i} \tag{10}$$

$$\varphi^i = \frac{1 - \frac{1}{(1+r)^{n^i}}}{r} \tag{11}$$

$$\dot{M}_{C6A,xa} = \frac{\text{Extra electricity consumed by the BESS}}{J_o} \times \dot{M}^{A}_{C6A} \tag{12}$$

2.4. Optimization Problem. The MIQCP problem was coded in Pyomo[42,43] and solved with Gurobi.[44] In light of the large problem size, a tolerance of 0.1% was imposed on the lower and upper bounds. The problem was solved in a high-performance computer.[45] A memory size of 1.2 TB was requested for this optimization. It took ca. 18 h to find the globally optimal solution.

2.4.1. Objective Function. This optimization aims to find a maximum ANP_{C6A} instead of the maximum LPC_{C6A} to circumvent the nonlinear form of the objective function. ANP_{C6A} is defined by the annual revenue upon hexanoic acid subtracted by the OPEX and EAC^{plant} allocated to hexanoic acid; see eqs 13−15. The annual revenue is the product of the yearly production quantity and market prices of the main product.

$$ANP_{C6A} = \theta_{C6A}\dot{M}_{C6A} - AF_{C6A}(EAC^{plant} + OPEX) \tag{13}$$

$$EAC^{plant} = \sum_{1}^{m} EAC^i + \frac{WC}{\varphi^{plant}} \tag{14}$$

$$\varphi^{plant} = \frac{1 - \frac{1}{(1+r)^{n^{plant}}}}{r} \tag{15}$$

The optimization variables were the scheduling profile and the size of the buffering units. The scheduling profile is composed of electricity stored into the BESS "Jin^F_t", electricity from the hybrid farms that is directly consumed by the plant excluding the BESS "J^F_t", intermediate chemicals stored into the ST "Lin^F_t", intermediate chemicals directly sent to the DSP from the MES "L^F_t", and intermediate chemicals sent to the DSP from the ST "$Lout^F_t$" (see in Figure 1b). The size of buffering units were "V_{BESS}" and "V_{ST}". Therefore, the objective function (i.e., eq 16) could be formulated based on eq 13 as

$$\max_{V_{BESS}, V_{ST}, Jin^F_t, J^F_t, Lin^F_t, L^F_t, Lout^F_t, X^F_t} \theta_{C6A} \sum_{t\in T} X^F_t - AF_{C6A}(EAC^{plant} + OPEX^F)$$
$$\forall\, t \in T \quad T = [1, 8760] \cap \mathbb{Z} \tag{16}$$

where all the variables are continuous.

2.4.2. Constraints. The electricity consumption rate (of the more flexible section of plant) "$J^F_t + Jout^F_t$" (GJ/h) was between 0 and its nominal rate "J_o" (GJ/h); see eq 17. The throughput rate of the DSP "$L^F_t + Lout^F_t$" (m^3/h) should be between 70 and 100% of its nominal rate "L_o" (m^3/h) or shutdown of the production "$L^F_t + Lout^F_t = 0$"; see eq 18. Moreover, the electricity consumption rate of the whole plant "$J^F_t + Jin^F_t$" (GJ/h) cannot be larger than the power supply "P^H_t" (GJ/h) or the plant's nominal capacity "J_o" (GJ/h); see eq 19. Time spent for ramping, starting up, and shutting down were neglected.

$$0 < J^F_t + Jout^F_t \le J_o \quad \forall\, t \in T \tag{17}$$

$$0.7 \le \frac{L^F_t + Lout^F_t}{L_o} \le 1 \vee L^F_t + Lout^F_t = 0 \quad \forall\, t \in T \tag{18}$$

$$0 < J^F_t + Jin^F_t \le P^H_t \quad \forall\, t \in T \tag{19}$$

Since eq 18 is a disjunctive constraint that can increase computational demand, a binary variable γ_t was introduced to define this constraint, which is the only binary variable in this optimization; see eq 20.

$$0.7\gamma_t \le \frac{L^F_t + Lout^F_t}{L_o} \le \gamma_t \quad \gamma_t \in \{0, 1\} \quad \forall\, t \in T \tag{20}$$

Two adjacent pieces of equipment should have the same load ratio. Taking into account that for each equipment its throughput rate is linear to its electricity consumption rate, the equations can be written as eqs 21 and 22

https://doi.org/10.1021/acs.iecr.4c01385
Ind. Eng. Chem. Res. 2024, 63, 17236−17251

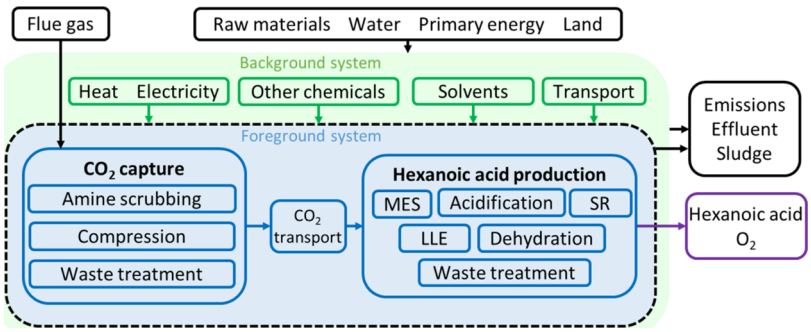

Figure 2. Product system. MES: microbial electrosynthesis. SR: solvent regeneration. LLE: liquid−liquid extraction.

$$\frac{J_t^F + \mathrm{Jout}_t^F}{J_o} = \frac{L_t^F + \mathrm{Lin}_t^F}{L_o} \quad \forall\, t \in T \tag{21}$$

$$\frac{L_t^F + \mathrm{Lout}_t^F}{L_o} = \frac{X_t^F}{X_o} \quad \forall\, t \in T \tag{22}$$

Further, it was assumed that at $t = 1$ the ST was full. Therefore, the cumulative quantity of the intermediate stream stored into or used from the ST at any time "t" should not exceed the maximum capacity of the ST "V_{ST}"; see eq 23. The same rationale was applied to the BESS as in eq 24.

$$-V_{ST} \le \sum_{1}^{t} (\mathrm{Lin}_t^F + \mathrm{Lout}_t^F) \le 0 \quad \forall\, t \in T \tag{23}$$

$$-V_{BESS} \le \sum_{1}^{t} (\mathrm{Jin}_t^F + \mathrm{Jout}_t^F) \le 0 \quad \forall\, t \in T \tag{24}$$

Moreover, filling "Lin_t^F" or draining "Lout_t^F" the ST could not occur simultaneously. The same applies to the BESS. Equations 25 and 26 exhibit nonlinearity. Usually, it can be avoided by introducing binary variables and combining them with the prefixed capacities of the buffering units.[27] However, the capacities of BESS and ST were also variables in this context. Hence, the nonlinearity of eqs 25 and 26 was kept.

$$\mathrm{Lin}_t^F \mathrm{Lout}_t^F = 0 \quad \forall\, t \in T \tag{25}$$

$$\mathrm{Jin}_t^F \mathrm{Jout}_t^F = 0 \quad \forall\, t \in T \tag{26}$$

2.4.3. Cost Functions. Equation 27 shows a general example of a cost function of storage tanks. Unlike "CAPEX^{BESS}", which is usually linear to the BESS capacity, "CAPEX^{ST}" presents a nonlinear relation to the size of the ST "V_{ST}".[37−39] This eventually introduces nonlinearity into the objective function. Therefore, underpinned by the results of the explorative case studies, the range of possible optimal size of ST could be narrowed down, and eq 27 could be linearized to eq 28. "α", "β", "λ", "η", "ω", and "ε" are constants (exact values can be found in SI)

$$\mathrm{CAPEX}^{ST} = \alpha(\beta + \lambda V_{ST}^{\eta}) \tag{27}$$

$$\mathrm{CAPEX}^{ST} = \omega V_{ST} + \varepsilon \tag{28}$$

Moreover, for the "OPEX^F", as shown in ref 21, nonlinearities exist between the utility consumption and production rate of hexanoic acid because of the penalties in utility usage due to flexible operation. This nonlinear relation would introduce another binary variable into the optimization, enlarging the optimization size and slowing down the calculation. Therefore, given that the penalties in utility consumption were negligible compared the plant's total consumption, the utility cost was linearized to the production rate based on the plant's nominal conditions (see eq 29).

$$\mathrm{OPEX}^F = (E^A + F^A + WT^A + UT^A)\frac{\sum_{t\in T} X_t^F}{\sum_{t\in T} X_t^A} + O\&M^F \quad \forall\, t \in T \tag{29}$$

2.5. Carbon Footprint Accounting. *2.5.1. Goal and Scope Definition.* A cradle-to-gate system boundary was chosen. The global warming potential (GWP) was evaluated for Cases A and B (reference cases) and F (optimized case). Carbon emissions related to facility and infrastructure were neglected in this work, assuming that the capital goods only account for a small portion of carbon emissions.[46]

2.5.2. Functional Unit and Allocation Method. The functional unit selected was 1 tonne of hexanoic acid produced. As oxygen was also produced, and to be consistent with the technoeconomic assessment, an economic allocation of emissions was used.

2.5.3. Product System. Figure 2 depicts the product system. The foreground system comprises three activities: CO_2 capture, CO_2 transport, and the hexanoic acid production. The CO_2 capture activity was not simulated in this work. It was assumed that the MES plant was located in the Port of Rotterdam, which is the initiator of a CO_2 transport and storage project − Porthos. Additionally, the leading CO_2 emitter in the Porthos project are integrated oil refineries.[47] Hence, it was assumed that the CO_2 capture facility was placed at these emission points. CO_2 is separated from the postcombustion flue gas by chemical absorption using monoethylamine (MEA).[47] Therefore, in the foreground system, the CO_2 capture activity consists of amine scrubbing, CO_2 compression, and waste treatment (nonrecycled solvent and water). After CO_2 is purified and compressed at the emission points, CO_2 is transported using the CO_2 network at the Port of Rotterdam. It is assumed that the MES plant can source purified and compressed CO_2 on demand from the pipeline network. Emissions from the pipeline transport of CO_2 were neglected. Moreover, it was assumed that the CO_2 conditions after transportation fulfilled MES unit requirements (i.e., no further CO_2 purification unit was needed in the plant).[48,49]

The end use of the products and solid waste generated in the foreground system was outside the system boundaries of this study. The reason for making this assumption for the solid waste was that it is mainly $CaHPO_4$ and can be recycled and

https://doi.org/10.1021/acs.iecr.4c01385
Ind. Eng. Chem. Res. 2024, 63, 17236−17251

treated for biomedical applications.[50] Meanwhile, the background system consists of the production of the solvent, other chemicals, and heating (incl. chilling) energy, electricity, infrastructure, and transport. Note that emissions from the original source of CO_2 were not included, assuming that the carbon emissions incurred during the production of flue gas are 100% allocated to the target products of the oil refineries.[51]

Process data of hexanoic production were taken from the resulting mass and energy balances of the Aspen process model. Process data of CO_2 capture was retrieved from.[47,52] The emission data of background system and elementary flows were retrieved from Ecoinvent[53] via SimaPro. Note that there are no data for $Ca(OH)_2$ and trioctylamine (TOA). Therefore, similar chemical or solvent were used as analogous. Complete process data and life cycle inventory data are presented in the SI.

2.6. Sensitivity Analyses. In the economic sensitivity analysis, the influence of five parameters on the LPC_{C6A} was analyzed for the optimized Case F, as listed in Table 2. A second sensitivity analysis was carried out to investigate the impact of the carbon intensity of the electricity grid and utility on the GWP in Cases A and F. It was assumed that the future electricity grid and utility would be defossilized by 90%. A third sensitivity analysis was done on the allocation method of GWP for Cases A, B and F. Mass allocation was applied.

Table 2. Input for Economic Sensitivity Analysis[a]

	low	high
CAPEX of MES, $CAPEX^{MES}$ (M€)	×10%	×200%
CAPEX of LLE, $CAPEX^{LLE}$ (M€)	×10%	×200%
CAPEX of ST, $CAPEX^{ST}$ (M€)	×10%	×200%
selling price of hexanoic acid, θ_{C6A} (€/kg)	−1	+1
interest rate, r	−0.05	+0.05

[a]Low and high inputs were obtained by multiplying a factor or adding or subtracting a value based on the initial inputs.

3. RESULTS AND DISCUSSION

3.1. Reference Cases. The annual production in Case A was 10 kt/y, and the resulting LPC_{C6A} was ca. 4.0 €/kg. In Case B (see Table 3), as no storage was deployed, the plant's volume flexibility remained as [70%, 100%]. As a result, the plant was shut down 2678 h. The drop in annual production was over 30%, and LPC_{C6A} was penalized by 19%.

3.2. Explorative Case Studies. *3.2.1. Cases C and D.* The key results are summarized in Table 3 and Figure 3. In Case C, where a BESS was implemented, a capacity of 1666 GJ/h (=463 MW) was sufficient to manage the periods with electricity shortage (Case B), implying a LRR of [0%,100%] for the whole plant during a year. The resulting production of hexanoic acid was 8.43 kt/y. This corresponds to 83% of the amount produced in Case A. In Case D, where a ST was installed, a size of 1964 m^3 was necessary to enable production without shutting down the plant. The resulting production of hexanoic acid was 8.02 kt/y, 80% of the nominal production. The difference between 8.43 kt/y in Case C and 8.02 kt/y in Case D was caused by the fact that batteries can store surplus electricity to promote the overall production (electricity consumptions higher than the equivalent to 100% plant load) while storage tanks are limited by the 100% plant load. According to the LPC_{C6A} results, the plant with a ST was economically favored even though it produced less hexanoic acid. This was due to the big difference in the CAPEX between a ST and a BESS. Furthermore, compared to Case A (see Table 3), the LPC_{C6A} values of Cases C and D were still considerably higher.

Table 3. Results of Cases A to D[a]

	A	B
LRR^k	-	[70%, 100%]
production shutdown time per year (h/y)	0	2678
hexanoic acid production (kt/y)	10.12	6.73
levelized production cost of hexanoic acid LPC^k_{C6A} (€/kg)	3.96	4.70
	C (plant with a BESS)	D (plant with a ST)
buffering capacity to fully eliminate shutdown	1666 GJ/h (=463 MW)	1964 m^3
hexanoic acid production when no shutdown (kt/y)	8.43	8.02
LPC^k_{C6A} when no shutdown (€/kg)	21.10	4.74
min LPC^k_{C6A} (€/kg)	4.67	4.38
sizes of buffering unit	12 GJ/h (=3.3 MW)	43 m^3
production shutdown time (h/y)	1954	989
hexanoic acid production (kt/y)	7.30	8.01
EC^k_{ttl} per annum	65%	72%
EC^k_{spl} per annum	<0.01%	-

[a]BESS: battery energy storage system. ST: storage tank. LPC_{C6A}: leveled production cost of hexanoic acid. EC_{ttl}: cumulative electricity consumption. EC_{spl}: surplus electricity consumption.

The trends and values of annual production, annual shutdown hours, and cumulative electricity consumption per annum as the sizes of both buffering units increase were similar between Cases C and D (Figure 3). The increase or decrease of these three indicators plateaued when the size of buffering units was around 40 GJ/h (=11 MW) or 40 m^3, respectively. The plateaued production quantity was about 8 kt/y, 80% of the nominal production, and close to the production generated when the shutdown time was fully eliminated. The annual shutdown hours were reduced from 2678 to nearly 1000. The total electricity consumption per annum reached nearly 72% of total electricity available from the hybrid farms. In Case C, see Figure 3, the lowest LPC^C_{C6A} achieved using a BESS was slightly lower than 4.7 €/kg, with a corresponding BESS capacity of 12 GJ/h. On the other hand, in Case D, the lowest LPC^D_{C6A} achieved using a ST was 4.4 €/kg, with a corresponding ST volume of 43 m^3. It can be seen that even when the installed capacity of BESS was 50 GJ/h, the value of surplus electricity consumption was less than 0.3%. This result showed that the BESS was hardly used for storing surplus electricity, which should have been its advantage over a ST.

It can be concluded that a ST was a less expensive and equally effective buffering choice over a BESS. With an optimized scheduling, a ST should be used more efficiently to boost the production, the range of the variable "V_{ST}" in the optimization problem being smaller than 43 m^3, as shown in Figure 3.

3.2.2. Case E. Using the results in Case D as a starting point, Figure 4 shows the extra production of hexanoic acid required to pay back the cost of the BESS installed when a ST of 43 m^3 was installed. It was clear in Figure 4 that when such a ST was operated following the schemes explained in Section 2.2.5, making the BESS larger would not generate enough extra production to pay back its capital cost (Figure 4). According to

https://doi.org/10.1021/acs.iecr.4c01385
Ind. Eng. Chem. Res. 2024, 63, 17236−17251

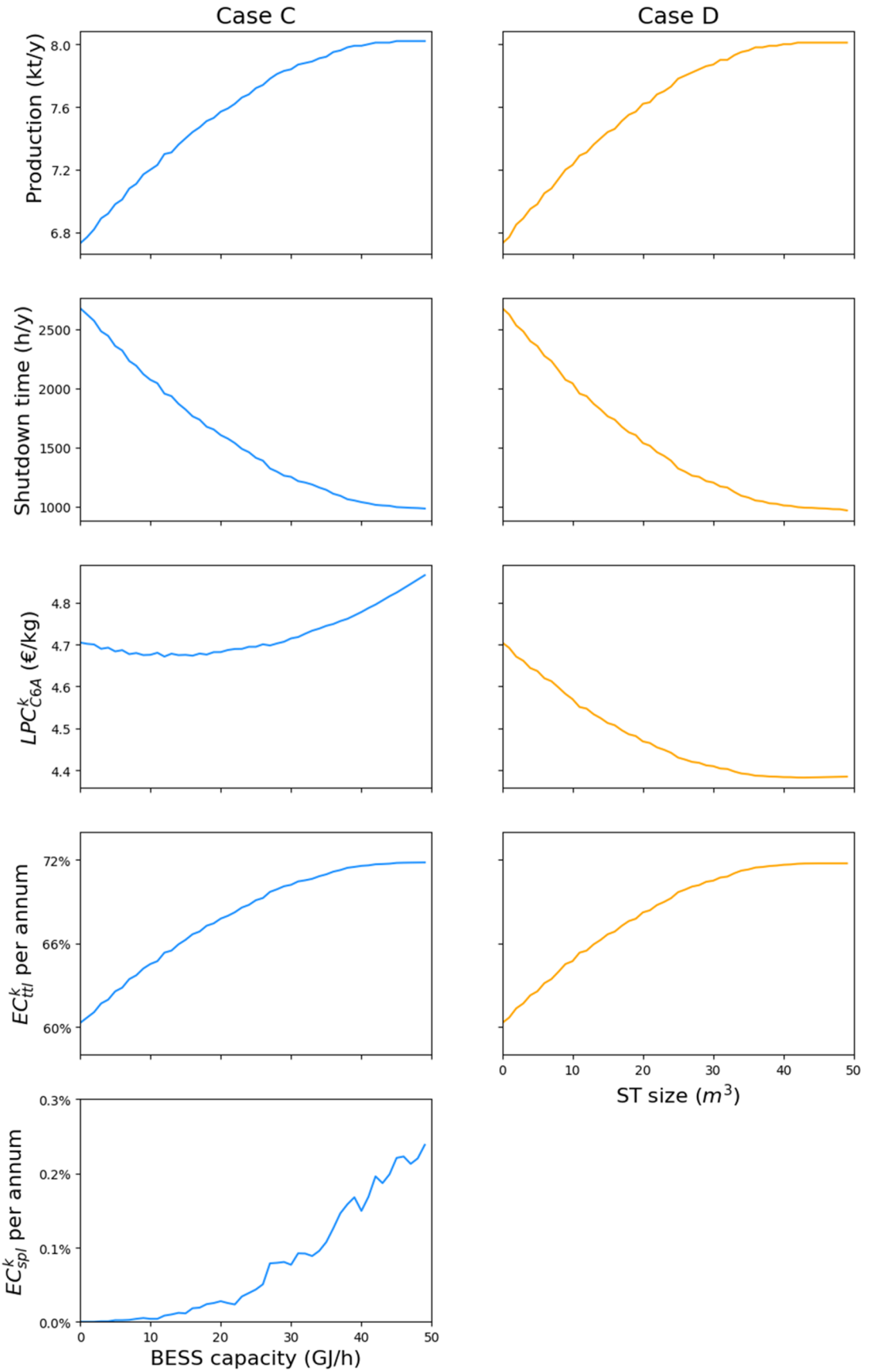

Figure 3. Results of the MES plant with a BESS and a ST individually (i.e., cases C and D, respectively) in production quantity of hexanoic acid, shutdown time, levelized production cost of hexanoic acid "LPC^{k}_{C6A}", total electricity consumption, "EC^{k}_{ttl}" per annum, and surplus electricity consumption "EC^{k}_{spl}" per annum.

https://doi.org/10.1021/acs.iecr.4c01385
Ind. Eng. Chem. Res. 2024, 63, 17236−17251

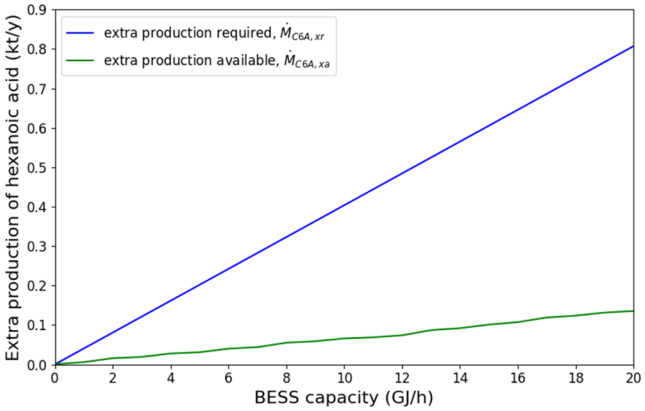

Figure 4. Extra production of hexanoic acid required to pay back the annualized capital investment in BESS versus extra production of hexanoic acid available per GJ/h of BESS installed in addition to a ST of 43 m^3.

the resulting operating profile of the BESS, the BESS was charged for 694 h and discharged for 716 h in a year. In the rest of the time, the BESS was not used. This could be a particular result of the electricity profile selected in the Rotterdam area and farms' size used in this case study, together with the size of the MES plant and BESS. Hence, in this context, the attempt to use BESS as much as possible for boosting the production failed; we could not equal 100% plant load during the whole year.

3.3. Optimized Case – Case F. Underpinned by the results of the explorative case studies, the optimization problem focused on the sizing and scheduling of the use of the ST only, and the BESS-related components (i.e., "Jin_t^F", "$Jout_t^F$", and "V_{BESS}") were not considered in the optimization.

The obtained optimal size of the storage tank was 35 m^3. The technoeconomic results of the optimized case (i.e., Case F) are summarized in Table 4. Cases A and B and D-ST35 and D-ST43 were used for comparison. D-ST35 is the subcase of Case D when the ST is 35 m^3, while D-ST43 is another subcase of Case D when the ST is 43 m^3. The following paragraphs compare and discuss these cases per indicator.

3.3.1. Shutdown Time and Production Quantity. In Case F, the plant's production shutdown time was 1152 h per year, which was more than halved upon Case B but still noticeably longer than in Case D-ST43 and especially Case D-ST35. However, the production quantity in Case F was slightly improved compared with Case D-ST35. This result proved that under the investigated conditions, a longer production shutdown time does not necessarily lead to less product or revenue. This finding can be explained by Figure 5 and electricity consumption conditions discussed in Section 3.3.3. Figure 5 is a snapshot of 24 h showing the available electricity from the hybrid farms and how Cases D-ST35 and F consumed the electricity for hexanoic acid production. The *Y*-axis values for Cases D-ST35 and F represent the sum of available electricity directly from hybrid farms and "stored electric energy" consumed in that specific hour (i.e., corresponding *x*-axis value). What is different between the two cases was that, in Case F, the production was more often promoted as soon as possible instead of being kept at 70% of the nominal production rate.

3.3.2. Load Ratio Range. Figure 6a shows the results of coverage percentage, how frequently the plant can be operated while consuming all the electricity supplied by the hybrid farms and producing hexanoic acid when the power supply from the hybrid farms is below 70% of the plant's nominal electricity consumption rate. The red dashed line marks the lower boundary of LRR. Left to this line, the plant cannot always use all the electricity supplied while producing hexanoic acid at the same time. In Case F, when the electricity supplied from the hybrid farms was between 60 and 100% of the plant's nominal electricity consumption rate, the plant could always use all the electricity supplied while safely producing hexanoic acid that meets requirements. The lower boundary of the LRR for Case F was lower than those for Cases D-ST35 and D-ST43. This was related to the steep slope in Case F when the electricity power was between 53 and 60% of the plant's nominal electricity consumption rate (see *X*-axis), and the coverage percentage dropped from 100 to 53% (see the left *Y*-axis). Given that in Figure 6b, the electricity consumption conditions for the three cases were similar when electricity power was between 53 and 60% of the plant's nominal electricity consumption rate, the slope in Case F shown in Figure 6a indicates that the plant shut down production more frequently than kept producing by using the intermediate chemicals stored in the ST. Such a slope was not found in either Cases D-ST35 or D-ST43, where the operating scheme was predetermined. This suggests that strategically shutting down production when facing larger shortages and bridging smaller shortages would enhance the volume flexibility of the plant.

3.3.3. Electricity Consumption. In Case F, the total electricity consumption per annum was 66%. Compared with Case D-ST35, it was enhanced by 2.2%. Meanwhile, it was only 0.4% lower than that in Case D-ST43, which is an insignificant decrease. Since the plant with a ST would never consume electricity beyond its nominal electricity load, the difference in total electricity consumption resulted from the consumption when the ratio of available electricity from the hybrid farms and nominal electricity consumption was below 70%. The total electricity consumption summed by different electricity loads below 70% is shown in Figure 6b. It can be deduced that a smaller ST with better scheduling could perform reasonably well compared with a larger ST operating under a specific predefined operating scheme, which was an educated guess based on the results of volume flexibility of the reference case.

Table 4. Comparison of the Cases[a]

	A	B	D-ST35	D-ST43	F
shutdown time per year (h/y)	0	2678	1075	989	1135
hexanoic acid production (kt/y)	10.12	6.73	7.96	8.01	8.00
LPC_{C6A}^k (€/kg)	3.96	4.70	4.39	4.38	4.37
LRR^k	-	[70%,100%]	[70%,100%]	[67%,100%]	[60%,100%]
EC_{ttl}^k per annum	100%	60.3%	63.8%	66.4%	66.0%

[a]LRR: load ratio range. LPC_{C6A}: levelized production cost of hexanoic acid. EC_{ttl}: total electricity consumption.

https://doi.org/10.1021/acs.iecr.4c01385
Ind. Eng. Chem. Res. 2024, 63, 17236−17251

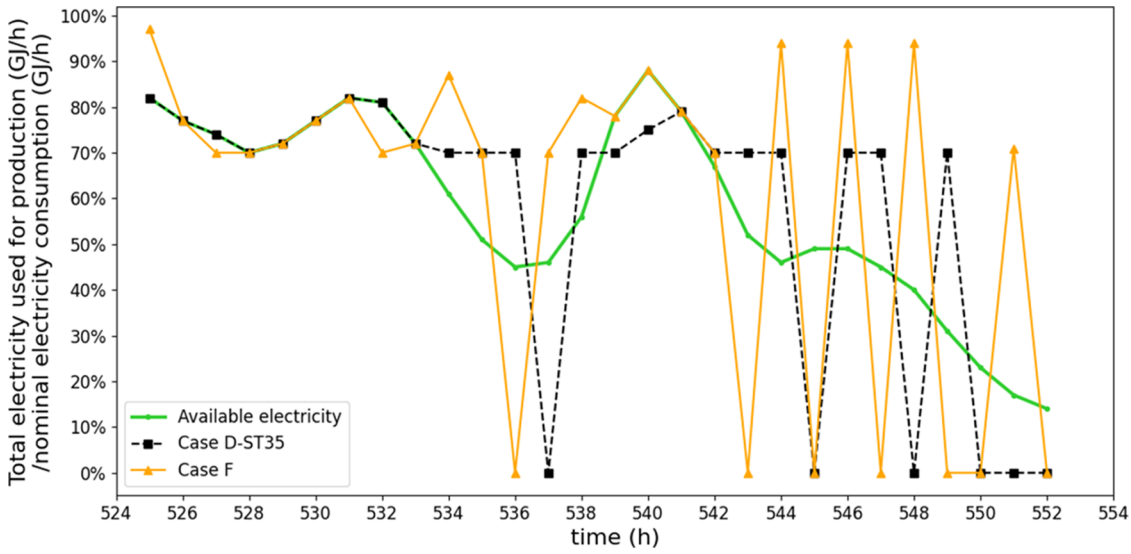

Figure 5. Illustration of production promotion by optimized scheduling. A snapshot of a day.

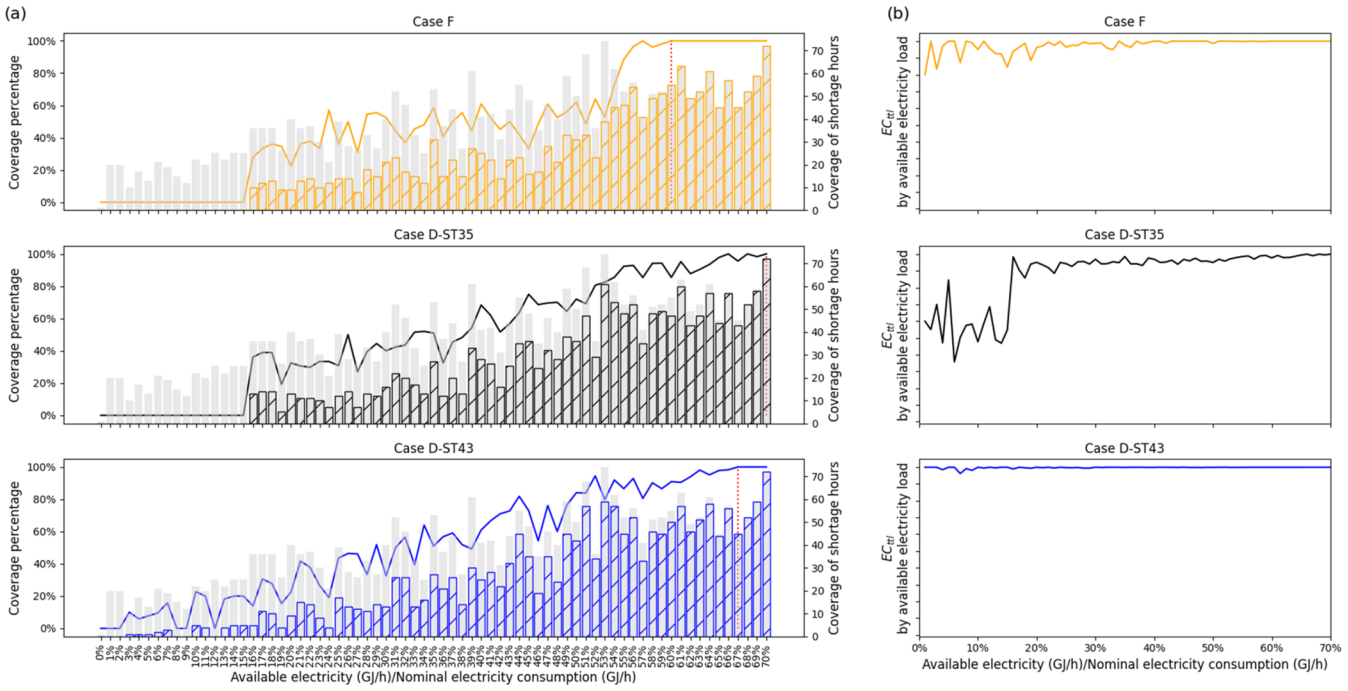

Figure 6. (a) Coverage percentage at electricity generated by the hybrid farms over nominal electricity consumption. Gray bars: number of hours in a year at a electricity power generated by the hybrid farms. Hatched bars: number of hours operated while meeting the expectations at an electricity power generated by the hybrid farms. Solid line: coverage percentage. Red dashed line: lower boundary of the LRR. (b) Total electricity consumption by an available electricity load generated by hybrid farms.

Since the production quantity was highly associated with the electricity consumption conditions, the results here confirm the finding in Section 3.3.1 that a longer production shutdown did not necessarily result in lower production.

3.3.4. Levelized Production Cost. The LPC^{F}_{C6A} is 4.4 €/kg, which is lower than in Case B but is higher than in Case A as well as the current market price of hexanoic acid (i.e., 2.5−4.2 €/kg[40]). Unexpectedly, LPC^{F}_{C6A} is similar to $LPC^{D\text{-}ST43}_{C6A}$ and $LPC^{D\text{-}ST35}_{C6A}$. The reasons are the minor increment in production quantity and the moderate decrease in the storage tank size. The breakdown of LPC^{A}_{C6A}, LPC^{B}_{C6A}, and LPC^{F}_{C6A} is shown in Figure 7a. When Cases B and F are compared with Case A, the total amount of capital cost related items (i.e., CAPEX and O&M) increased while the total amount of operation related items (i.e., the rest items) decreased. The trend was reversed when comparing Case F to Case B. This indicates that, shifting from constant electricity supply to hybrid IRE leads to less output and thus less revenue and eventually a higher sunk cost in the capital items. Implementing a ST helped reducing the impact, though to a minor extent.

3.3.5. Carbon Footprint. As can be seen in Figure 7b, Cases B and F exhibit similar GWPs, around 5.3 t of CO_2eq/t of C6A, which indicates that the impact of linearization of utility consumption on GWP is negligible. Moreover, Figure 7b shows that the GWP of Case F was 2.8 times lower than that of

https://doi.org/10.1021/acs.iecr.4c01385
Ind. Eng. Chem. Res. 2024, 63, 17236−17251

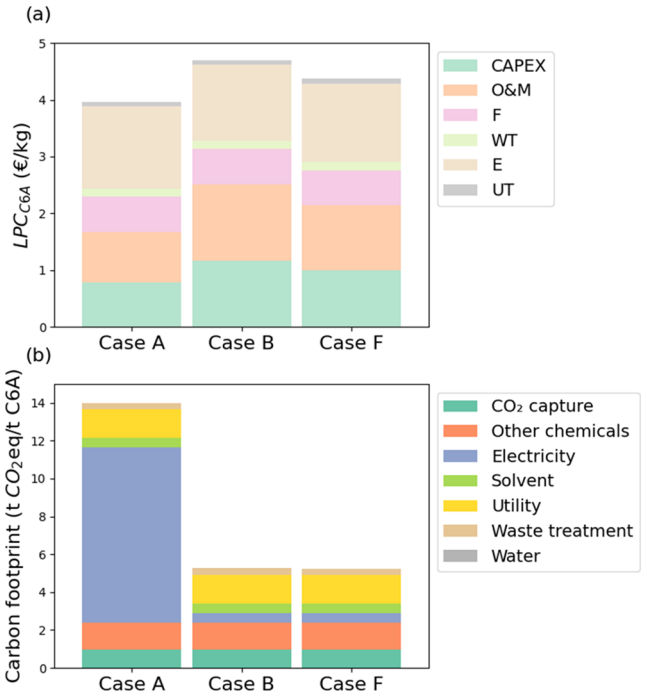

Figure 7. (a) Breakdown of the leveled production cost of hexanoic acid in Cases A, B, and F. CAPEX: capital expenditure. O&M: operation and maintenance. F: feedstock. WT: waste treatment. E: electricity. UT: utility. (b) Carbon footprint and their breakdown for Cases A, B and F with an economic allocation.

Case A, which is credited to the coupling between the MES plant and hybrid IRE.

In all three cases, the CO_2 capture process led to an emission of 1.0 t CO_2eq/t C6A. Since the CO_2 used for hexanoic acid production as feedstock was 2.2 t CO_2/t C6A, the carbon intensity of capturing CO_2 is up to 0.4 t CO_2eq/t CO_2 captured. However, in Case A, the CO_2 capture process was only responsible for 7% of total emissions, while in Cases B and F, it constituted 19% of the total emissions as a result of the change in electricity source. In Case A, the highest share of emissions were attributed to electricity generation, utilities generation, and other chemicals' syntheses. In both Cases B and F, the three largest contributors were utilities generation, production of other chemicals, and electricity generation. This was due to the energy-intensive nature of the DSP and the use of fossil-based chemicals and solvents.

3.3.6. Sensitivity Analyses. 3.3.6.1. Economic. The results of the economic sensitivity analysis are shown in Figure 8a. The impact of changes in parameters on LPC^{F}_{C6A} were almost linear to the changes in the variables, except for the $CAPEX^{MES}$ and θ_{C6A}. This is caused by the resulting positive operating income and the consequent tax. $CAPEX^{MES}$, makes up 50% of the CAPEX of all equipment. Therefore, lowering its cost not only reduced the initial capital expenditures of the plant but also the annual O&M. This, in turn, increased the annual operating income, which became positive. It was similar for the θ_{C6A}. The original θ_{C6A} was not sufficient for the plant to achieve a positive operating income. As the selling price increased and thus the revenue increased, the plant's operating income turned positive. In both situations, the resulting operating income fell in the high-tax range in The Netherlands (see SI for tax details). As a result, the operating costs increased, and the LPC^{F}_{C6A} became higher than expected. This

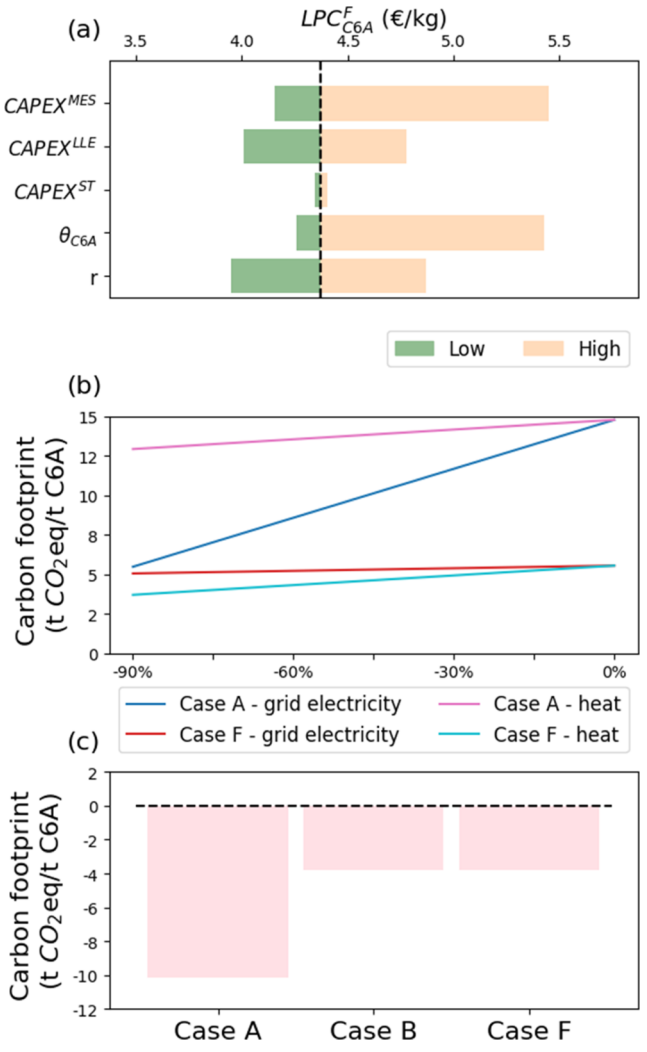

Figure 8. (a) Results of the economic sensitivity analysis. $CAPEX^{MES}$: capital cost of the microbial electrosynthesis unit. $CAPEX^{LLE}$: capital cost of the liquid−liquid extraction units. $CAPEX^{ST}$: capital cost of the storage tanks. θ_{C6A}: selling price of hexanoic acid. *r*: interest rate. (b) Sensitivity analysis on the carbon intensity of grid electricity and utility (incl. chilling energy). (c) Change in carbon footprint from original results that used economic allocation versus mass allocation.

change induced by tax did not occur with the $CAPEX^{LLE}$, because its decrease was not enough to enable a positive operating income.

3.3.6.2. Carbon Footprint. The results of the sensitivity analysis on the emission intensity of grid electricity and utility in Cases A and F are shown in Figure 8b. Case A was more sensitive to the changes in emission intensity of grid electricity while Case F was more sensitive to that of utility energy. In Case A, only grid electricity was supplied throughout the supply chain, which was the highest emitter. Hence, it makes sense that decarbonizing the grid electricity posed a higher impact. In Case F, utility, which was generated from natural gas, emitted the most. Electricity consumed in the MES plant was already from renewables and thus provides less opportunity for further decarbonization. Therefore, the observation from this sensitivity analysis, again, suggested that electricity should no longer be seen as a defossilising focus if further defossilisation is expected for a MES plant coupled with hybrid IRE.

https://doi.org/10.1021/acs.iecr.4c01385
Ind. Eng. Chem. Res. 2024, 63, 17236−17251

Regarding allocation, using mass allocation instead of economic allocation lowered the GWP by two-thirds based on the GWP that was obtained with economic allocation (see Figure 8c). In Case F, the GWP allocated to liquid oxygen would change from 0.3 t CO_2eq/t O_2 to 1.7 t CO_2eq/t O_2. Note that the current GWP per tonne of liquid oxygen generated by an air separation unit in Europe is around 0.6 t CO_2eq/t O_2.[53] Usually, with mass allocation, the technical improvement of the technologies or processes that lead to an increased mass ratio of the main products is more visible.[54] Nonetheless, in the MES plant, the mass ratio between hexanoic acid and oxygen always remains the same. Therefore, this advantage of mass allocation does not apply in this context. On the other hand, mass allocation is more reliable when the market price of the (by)products change over time.[54] Therefore, the employment of mass allocation will be sensible if the amount of oxygen produced via MES becomes much more indispensable in the market or if the prices of the two products become more volatile over time.

4. CONCLUSIONS

This work has investigated how intermittency affects the sizing of the buffering units and scheduling of a novel MES plant, designed to produce 10 kt/y at continuous and full load, and what the trade-offs are in terms of economic performance and carbon emissions. First, explorative case studies were conducted to simplify the optimization problem. Then, a MIQCP problem was proposed to optimize the scheduling profiles and the size of a ST, seeking the maximum ANP_{C6A}. Last, technoeconomic and environmental performances of the optimized case, compared to relevant explorative case studies, were assessed.

Concluding from the explorative studies, a storage tank was found to be more economical than a BESS to buffer fluctuations in available electricity from the hybrid farms when the load was between 0 and 100% of the plant's nominal consumption rate. A BESS had a limited advantage in consuming surplus electricity when the available electricity supply from the hybrid farms was over 100% of the MES's plant nominal capacity. Additionally, the deployment of BESS had a high impact on the CAPEX of the plant when its capacity was larger than 12 GJ/h (=3.3 MW). Hence, an ST was in a better position to foster the economic potential of the MES plant. With the help of a ST of 43 m^3, available electricity that was below 100% of the plant's nominal consumption rate could be nearly completely used by the MES plant while the levelized production cost of hexanoic acid was lowered compared to the ST-free case. As a result, this work considered only the ST in the optimization. The resulted optimal size of the ST was 35 m^3.

When compared to the case where the operating scheme of the ST was predefined, the optimal scheduling profile suggested (1) the plant stops producing hexanoic acid and store the intermediate chemicals when the available electricity from the hybrid farms was below 60% of the plant's nominal electricity consumption and (2) the intermediate chemicals stored to promote production should be used as soon as possible. This practice also enhanced the volume flexibility, expanding the load ratio range from [70%, 100%] to [60%, 100%]. However, the leveled production cost was not significantly reduced, because both the reduction in CAPEX and the increase in revenue were marginal. These indicate that even with the cheaper solution-storage tanks plus additional optimal scheduling, the flexibility and economic viability of the MES plant could not be sufficiently improved due to the DSP technologies. To make the MES technology more attractive for flexible operation, it should be coupled with more flexible DSP technologies or improved product concentration to circumvent downstream processing with flexibility constraints, such as distillation.

Moreover, even with an optimal size of ST and an optimal scheduling profile, the MES plant powered with the selected hybrid IRE was still less economically favorable compared to the case when it was powered by a constant grid electricity. However, from an environmental point of view, the MES plant running on the hybrid IRE outperformed the MES plant with constant grid electricity. The cradle-to-gate carbon emissions became 2.8 times lower as the substantial amount of electricity the MES demanded was replaced by hybrid renewable IRE. The results show that using grid electricity is not an option unless it is further decarbonized. Moreover, the impact of penalties on energy consumption induced by flexible operation was minor. The results also show that in the MES plant powered by hybrid IRE, utility energy, solvent and other chemicals were the major CO_2 emitters. To further defossilize the MES-based system, utilities, solvents, and other chemicals would need to be produced from nonfossil sources.

As for limitations, this study did not include ramping, starting-up, and shutting-down procedures, and the assumed charging and discharging rates of the BESS were highly optimistic. Taking these factors into account may affect the results for the BESS, because the stored electricity could possibly be used to prevent the plant from being completely shut down. The low potential for BESS was also compounded by the fact that the electricity profile and pricing scheme were highly specific, though reasonable. Perhaps the advantage of BESS would be more visible under other pricing schemes[27] or electricity profiles with a more alternating pattern. To enable a more efficient optimization, the nonlinearities could be linearized to avoid a large memory demand. Given the low TRL of the technology, many hypotheses were considered in the plant modeling. As the technology advances, the proposed model of the MES unit and the plant should be updated, also to incorporate operation under a variable electricity profile; validation of operation under IRE in a lab or pilot plant setup would be needed. Moreover, with the possibility to scale up the global market of hexanoic acid due to future applications such as blends for sustainable aviation fuels,[55] it is important to investigate the environmental burdens of the full value chain. A comprehensive life cycle assessment should be performed to understand the environmental performances from a broader perspective.

■ ASSOCIATED CONTENT

Supporting Information

The Supporting Information is available free of charge at https://pubs.acs.org/doi/10.1021/acs.iecr.4c01385.

Electricity profiles; inputs for technoeconomic assessment; operating schemes; process data; life cycle inventory; hypothesis check (PDF)

■ AUTHOR INFORMATION

Corresponding Author

Jisiwei Luo − *Department of Engineering Systems and Services, Faculty of Technology, Policy and Management, Delft*

https://doi.org/10.1021/acs.iecr.4c01385
Ind. Eng. Chem. Res. 2024, 63, 17236−17251

University of Technology, 2628 BX Delft, The Netherlands; orcid.org/0000-0003-0935-3315; Email: J.Luo-1@tudelft.nl

Authors

Mar Pérez-Fortes − *Department of Engineering Systems and Services, Faculty of Technology, Policy and Management, Delft University of Technology, 2628 BX Delft, The Netherlands;* orcid.org/0000-0002-1132-4014

Adrie J. J. Straathof − *Department of Biotechnology, Faculty of Applied Sciences, Delft University of Technology, 2629 HZ Delft, The Netherlands;* orcid.org/0000-0003-2877-4756

Andrea Ramirez − *Department of Chemical Engineering, Faculty of Applied Sciences, Delft University of Technology, 2629 HZ Delft, The Netherlands*

Complete contact information is available at: https://pubs.acs.org/10.1021/acs.iecr.4c01385

Notes

The authors declare no competing financial interest.

■ ACKNOWLEDGMENTS

This work was supported by Shell and a PPP-allowance from Top Consortia for Knowledge and Innovation (TKI's) of the Dutch Ministry of Economic Affairs and Climate Policy in the context of the TU Delft e-Refinery Institute.

■ NOMENCLATURE

Vectors

C_v	Yearly coverage percentage of shortage hours at an available electricity power v,%
Lin_t	Intermediate chemicals stored into the storage tank at time t, m^3/h
Lout_t	Intermediate chemicals sent to the DSP units from the storage tank at time t, m^3/h
L_t	intermediate chemicals directly sent to the DSP from the MES at time t, m^3/h
Jin_t	electricity stored in the BESS at time t, GJ/h
Jout_t	electricity discharged from the BESS at time t, GJ/h
J_t	electricity consumption immediately used for hexanoic acid production at time t, GJ/h
P_t^{H}	available electricity from the hybrid farms (i.e., wind and solar) at time t, GJ/h
T	time vector, 1−8760 h
V	vector of hourly available electricity over hourly nominal electricity consumption (for intermediate calculation), %
X_t	production of hexanoic acid at time t, kt/h
γ_t	binary variable

Symbols

E	electricity price, M€/y
F	feedstock price, M€/y
J	electricity consumption, GJ/h
$\dot{M}$	mass flow rate at plant level, kt/y
m	total number of equipment
n	plant lifetime, years
r	discount rate, %
UT	utility price at plant level, M€/y
v	available electricity power generated by the wind and/or solar farm (time-independent), GJ/h
v^*	available electricity power generated by the wind and/or solar farm (time-independent; for intermediate calculation), GJ/h
WT	waste treatment price, M€/y
$\mathbb{Z}$	Integers
θ	price, €/kg
φ	annuity factor
Φ	statement inside the Iverson bracket
α	constant
β	constant
λ	constant
η	constant
ω	constant
ε	constant

Superscripts

i	type of equipment
k	case number, from A to F

Subscripts

C6A	hexanoic acid
LB	lower boundary
max	maximum value
min	minimum value
o	nominal value
O_2	oxygen
t	time, h
UB	upper boundary
y	year
xa	extra available
xr	extra required

Acronyms

AF	allocation factor
ANP	annualized net profit, M€/y
BESS	battery energy storage system
CAPEX	capital expenditure, M€/y
DSP	downstream processing
EAC	equivalent annualized price, M€/y
IRE	intermittent renewable electricity
LLE	liquid−liquid extraction
LPC	levelized production cost, €/kg
LRR	load ratio range, %
MES	microbial electrosynthesis
MILP	mixed-integer linear programming
MINLP	mixed-integer nonlinear programming
MIQCP	mixed-integer quadratically constrained programming
O&M	operation and maintenance price, M€/y
OPEX	operating expenditure, M€/y
SI	Supporting Information
SR	solvent regeneration
ST	storage tank
TD	dehydration column
TOA	trioctylamine
WC	working capital, M€

■ REFERENCES

(1) Osman, O.; Sgouridis, S.; Sleptchenko, A. Scaling the production of renewable ammonia: A techno-economic optimization applied in regions with high insolation. *J. Clean. Prod.* **2020**, *271*, No. 121627.

(2) Breyer, C.; Bogdanov, D.; Gulagi, A.; Aghahosseini, A.; Barbosa, L. S. N. S.; Koskinen, O.; Barasa, M.; Caldera, U.; Afanasyeva, S.; Child, M.; et al. On the role of solar photovoltaics in global energy transition scenarios. *Prog. Photovoltaics* **2017**, *25* (8), 727−745.

(3) Chung, W.; Jeong, W.; Lee, J.; Kim, J.; Roh, K.; Lee, J. H. Electrification of CO2 conversion into chemicals and fuels: Gaps and opportunities in process systems engineering. *Comput. Chem. Eng.* **2023**, *170*, No. 108106, DOI: 10.1016/j.compchemeng.2022.108106.
(4) Burre, J.; Bongartz, D.; Brée, L.; Roh, K.; Mitsos, A. Power-to-X: Between Electricity Storage, e-Production, and Demand Side Management. *Chem. Ing. Tech.* **2020**, *92* (1−2), 74−84.
(5) Prévoteau, A.; Carvajal-Arroyo, J. M.; Ganigue, R.; Rabaey, K. Microbial electrosynthesis from CO(2): forever a promise? *Curr. Opin. Biotechnol.* **2020**, *62*, 48−57.
(6) Jourdin, L.; Grieger, T.; Monetti, J.; Flexer, V.; Freguia, S.; Lu, Y.; Chen, J.; Romano, M.; Wallace, G. G.; Keller, J. High Acetic Acid Production Rate Obtained by Microbial Electrosynthesis from Carbon Dioxide. *Environ. Sci. Technol.* **2015**, *49* (22), 13566−13574.
(7) Sadhukhan, J.; Lloyd, J. R.; Scott, K.; Premier, G. C.; Yu, E. H.; Curtis, T.; Head, I. M. A critical review of integration analysis of microbial electrosynthesis (MES) systems with waste biorefineries for the production of biofuel and chemical from reuse of CO2. *Renewable Sustainable Energy Rev.* **2016**, *56*, 116−132.
(8) Canapi, E. C.; Agustin, Y. T. V.; Moro, E. A.; Pedrosa, E.; Bendaño, M. a. L. J. Coconut Oil. In *Bailey's Industrial Oil and Fat Products*, 6th ed.; Shahidi, F., Ed.; John Wiley & Sons, 2005; Vol. *1*−*6*, pp 123−147.
(9) Basiron, Y. Palm oil. In *Bailey's Industrial Oil and Fat Products*, 6th ed.; Shahidi, F., Ed.; John Wiley & Sons, 2005; Vol. *1*−*6*.
(10) Jouny, M.; Luc, W.; Jiao, F. General Techno-Economic Analysis of CO2 Electrolysis Systems. *Ind. Eng. Chem. Res.* **2018**, *57* (6), 2165−2177.
(11) Van Dael, M.; Kreps, S.; Virag, A.; Kessels, K.; Remans, K.; Thomas, D.; De Wilde, F. Techno-economic assessment of a microbial power-to-gas plant − Case study in Belgium. *Appl. Energy* **2018**, *215*, 416−425.
(12) Yang, E.; Omar Mohamed, H.; Park, S. G.; Obaid, M.; Al-Qaradawi, S. Y.; Castano, P.; Chon, K.; Chae, K. J. A review on self-sustainable microbial electrolysis cells for electro-biohydrogen production via coupling with carbon-neutral renewable energy technologies. *Bioresour. Technol.* **2021**, *320* (Pt B), No. 124363.
(13) Greenblatt, J. B.; Miller, D. J.; Ager, J. W.; Houle, F. A.; Sharp, I. D. The Technical and Energetic Challenges of Separating (Photo)Electrochemical Carbon Dioxide Reduction Products. *Joule* **2018**, *2* (3), 381−420.
(14) Savla, N.; Suman; Pandit, S.; Verma, J. P.; Awasthi, A. K.; Sana, S. S.; Prasad, R. Techno-economical evaluation and life cycle assessment of microbial electrochemical systems: A review. *Curr. Res. Green Sustainable Chem.* **2021**, *4*, No. 100111.
(15) Hernandez, P. A.; Zhou, M.; Vassilev, I.; Freguia, S.; Zhang, Y.; Keller, J.; Ledezma, P.; Virdis, B. Selective Extraction of Medium-Chain Carboxylic Acids by Electrodialysis and Phase Separation. *ACS Omega* **2021**, *6* (11), 7841−7850.
(16) Angenent, L. T.; Richter, H.; Buckel, W.; Spirito, C. M.; Steinbusch, K. J.; Plugge, C. M.; Strik, D. P.; Grootscholten, T. I.; Buisman, C. J.; Hamelers, H. V. Chain Elongation with Reactor Microbiomes: Open-Culture Biotechnology To Produce Biochemicals. *Environ. Sci. Technol.* **2016**, *50* (6), 2796−2810.
(17) del Pilar Anzola Rojas, M.; Mateos, R.; Sotres, A.; Zaiat, M.; Gonzalez, E. R.; Escapa, A.; De Wever, H.; Pant, D. Microbial electrosynthesis (MES) from CO2 is resilient to fluctuations in renewable energy supply. *Energy Convers. Manage.* **2018**, *177*, 272−279.
(18) Del Pilar Anzola Rojas, M.; Zaiat, M.; Gonzalez, E. R.; De Wever, H.; Pant, D. Effect of the electric supply interruption on a microbial electrosynthesis system converting inorganic carbon into acetate. *Bioresour. Technol.* **2018**, *266*, 203−210.
(19) Diego-García, R.; Morán, A.; Romeo, L. M. Integration of oxycombustion and microbial electrosynthesis for sustainable energy storage. *Energy Convers. Manage.* **2022**, *269*, No. 116002, DOI: 10.1016/j.enconman.2022.116002.
(20) Mateos, R.; Escapa, A.; San-Martín, M. I.; De Wever, H.; Sotres, A.; Pant, D. Long-term open circuit microbial electrosynthesis system promotes methanogenesis. *J. Energy Chem.* **2020**, *41*, 3−6.
(21) Luo, J.; Pérez-Fortes, M.; Ibarra-Gonzalez, P.; Straathof, A. J. J.; Ramirez, A. Impact of intermittent electricity supply on a conceptual process design for microbial conversion of CO2 into hexanoic acid. *Chem. Eng. Res. Des.* **2024**, *205*, 364−375.
(22) Luo, J.; Moncada, J.; Ramirez, A. Development of a Conceptual Framework for Evaluating the Flexibility of Future Chemical Processes. *Ind. Eng. Chem. Res.* **2022**, *61* (9), 3219−3232.
(23) Layritz, L. S.; Dolganova, I.; Finkbeiner, M.; Luderer, G.; Penteado, A. T.; Ueckerdt, F.; Repke, J. U. The potential of direct steam cracker electrification and carbon capture & utilization via oxidative coupling of methane as decarbonization strategies for ethylene production. *Appl. Energy* **2021**, *296*, No. 117049, DOI: 10.1016/j.apenergy.2021.117049.
(24) Moioli, E.; Wotzel, A.; Schildhauer, T. Feasibility assessment of small-scale methanol production via power-to-X. *J. Clean. Prod.* **2022**, *359*, No. 132071.
(25) Qi, M.; Park, J.; Landon, R. S.; Kim, J.; Liu, Y.; Moon, I. Continuous and flexible Renewable-Power-to-Methane via liquid CO2 energy storage: Revisiting the techno-economic potential. *Renewable Sustainable Energy Rev.* **2022**, *153*, No. 111732.
(26) Salomone, F.; Giglio, E.; Ferrero, D.; Santarelli, M.; Pirone, R.; Bensaid, S. Techno-economic modelling of a Power-to-Gas system based on SOEC electrolysis and CO2 methanation in a RES-based electric grid. *Chem. Eng. J.* **2019**, *377*, No. 120233.
(27) Brée, L. C.; Bulan, A.; Herding, R.; Kuhlmann, J.; Mitsos, A.; Perrey, K.; Roh, K. Techno-Economic Comparison of Flexibility Options in Chlorine Production. *Ind. Eng. Chem. Res.* **2020**, *59* (26), 12186−12196.
(28) Barbosa-Póvoa, A.; Macchietto, S. Detailed design of multipurpose batch plants. *Comput. Chem. Eng.* **1994**, *18* (11−12), 1013−1042.
(29) Thomaidis, T. V.; Pistikopoulos, E. N. Optimal-Design of Flexible and Reliable Process Systems. *IEEE Trans. Reliab.* **1995**, *44* (2), 243−250.
(30) Schulte Beerbühl, S.; Fröhling, M.; Schultmann, F. Combined scheduling and capacity planning of electricity-based ammonia production to integrate renewable energies. *Eur. J. Oper. Res.* **2015**, *241* (3), 851−862.
(31) Zhang, Q.; Martín, M.; Grossmann, I. E. Integrated design and operation of renewables-based fuels and power production networks. *Comput. Chem. Eng.* **2019**, *122*, 80−92.
(32) Sánchez, A.; Martín, M. Optimal renewable production of ammonia from water and air. *J. Clean. Prod.* **2018**, *178*, 325−342.
(33) Varela, C.; Mostafa, M.; Zondervan, E. Modeling alkaline water electrolysis for power-to-x applications: A scheduling approach. *Int. J. Hydrogen Energy* **2021**, *46* (14), 9303−9313.
(34) Teichgraeber, H.; Brandt, A. R. Optimal design of an electricity-intensive industrial facility subject to electricity price uncertainty: Stochastic optimization and scenario reduction. *Chem. Eng. Res. Des.* **2020**, *163*, 204−216.
(35) Huesman, A. Integration of operation and design of solar fuel plants: A carbon dioxide to methanol case study. *Comput. Chem. Eng.* **2020**, *140*, No. 106836.
(36) Statista. *Prices of Electricity for Non-household Consumers in the Netherlands*. 2022. https://www.statista.com/statistics/596254/electricity-industry-price-netherlands/#:~:text=The%2010.51%20euro%20cents%20per,towards%20the%20middle%2Drange%20of (accessed 11 Nov 2022).
(37) Towler, G.; Sinnott, R. *Chemical Engineering Design: Principles, Practice and Economics of Plant and Process Design*; Butterworth-Heinemann, 2021.
(38) Max, S. P.; Klaus, D. T.; Ronald, E. W. *Plant Design and Economics for Chemical Engineers*; McGraw-Hill Companies, 2003.
(39) Sieder, W.; Seader, J.; Lewin, D. *Product and Process Design Principles*; John Wiley & Sons, 2004.

(40) Dessì, P.; Rovira-Alsina, L.; Sanchez, C.; Dinesh, G. K.; Tong, W.; Chatterjee, P.; Tedesco, M.; Farras, P.; Hamelers, H. M. V.; Puig, S. Microbial electrosynthesis: Towards sustainable biorefineries for production of green chemicals from CO(2) emissions. *Biotechnol. Adv.* **2021**, *46*, No. 107675.
(41) Intratec. *Oxygen Price | Current and Forecast*. 2022. https://www.intratec.us/chemical-markets/oxygen-price (accessed 20 Sept 2022).
(42) Hart, W. E.; Watson, J. P.; Woodruff, D. L. Pyomo: modeling and solving mathematical programs in Python. *Math. Program. Comput.* **2011**, *3* (3), 219−260.
(43) Bynum, M. L.; Hackebeil, G. A.; Hart, W. E.; Laird, C. D.; Nicholson, B. L.; Siirola, J. D.; Watson, J.-P.; Woodruff, D. L. *Pyomo — Optimization Modeling in Python*; Springer, 2021. DOI: 10.1007/978-3-030-68928-5.
(44) Gurobi Optimization Gurobi Optimizer Reference Manual. In *Gurobi Optimization*; LLC, 2023.
(45) DHPC. *DelftBlue Supercomputer (Phase 1)*; Delft High Performance Computing Centre (DHPC), 2022.
(46) Hauschild, M. Z.; Rosenbaum, R. K.; Olsen, S. I. *Life Cycle Assessment*; Springer, 2018. DOI: 10.1007/978-3-319-56475-3.
(47) IEAGHG. *Understanding the Cost of Retrofitting CO2 Capture in an Integrated Oil Refinery*; IEAGHG, 2017. http://documents.ieaghg.org/index.php/s/2cCda5q0bnYhsvo.
(48) Jourdin, L. *Personal Communication*. Luo, J., 2023.
(49) Porthos. *Porthos CO_2 specifications*. 2021. https://www.porthosco2.nl/wp-content/uploads/2021/09/CO2-specifications.pdf (accessed 05 Jan 2023).
(50) Tamimi, F.; Sheikh, Z.; Barralet, J. Dicalcium phosphate cements: brushite and monetite. *Acta Biomater.* **2012**, *8* (2), 474−487.
(51) European Commission. *LCA4CCU-Guidelines for Life Cycle Assessment of Carbon Capture and Utilisation*; European Commission: Brussels, 2020. DOI: 10.2833/161308.
(52) IEAGHG. *Techno - Economic Evaluation of SMR Based Standalone (Merchant) Hydrogen Plant with CCS*; IEAGHG, 2017. https://ieaghg.org/publications/techno-economic-evaluation-of-smr-based-standalone-merchant-hydrogen-plant-with-ccs/.
(53) Wernet, G.; Bauer, C.; Steubing, B.; Reinhard, J.; Moreno-Ruiz, E.; Weidema, B. The ecoinvent database version 3 (part I): overview and methodology. *Int. J. Life Cycle Assess* **2016**, *21* (9), 1218−1230.
(54) Pishgar-Komleh, S. H.; Vellinga, T. *Evaluation of Allocation Methods in Beef and Pork Production at Slaughterhouse Level*; Wageningen Livestock Research: Wageningen, 2022. DOI: 10.18174/576774.
(55) U.S. Department of Energy. *Sustainable Aviation Fuel: Review of Technical Pathways*; U.S. Department of Energy: United States, 2020. DOI: 10.2172/1660415.